



## **EXPERIMENTAL STUDY ON DEFORMATION CAPACITY OF REINFORCED CONCRETE CORE WALLS AFTER FLEXURAL YIELDING**

T. NAKACHI, T. TODA and K. TABATA

Technical Research Institute, HAZAMA Corporation, 515-1, Nishimukai, Karima,  
Tsukuba, Ibaraki, 305, Japan

### **ABSTRACT**

This paper describes the deformation capacity of multistory reinforced concrete core walls after flexural yielding. Lateral loading tests on four core walls were conducted. The test parameters were the concrete confinement at the corner, the amount of confining steel at the corner, and the area of concrete confinement. The compressive strength of the concrete used was approximately 60 MPa. To study the concrete confinement at the corner, compression tests were conducted on square and rectangular section columns in order to simulate the corner and the area near the corner respectively. The relationship between compressive ductility of the concrete at the corner and the deformation capacity of core walls was then determined.

### **KEYWORDS**

Deformation capacity; shear wall; high-strength; confinement effect; reinforced concrete; loading test

### **INTRODUCTION**

In a core wall system high-rise building, the center core of which consists of four L-shaped core walls, under the action of a diagonal seismic force(Fig. 1), the axial load of the core wall is very high. Particularly the corner and the area near the corner of the L-shaped core wall are subject to high compressive stress. Reinforcing these areas is therefore considered effective in improving the deformation capacity of the core walls. This paper examines the relationship between the degree of confinement or reinforcing of these areas and the deformation capacity of the core wall. Evaluation was based on the results of core wall lateral loading and compression tests.

### **LATERAL LOADING TEST OF CORE WALLS**

#### *Test Specimens*

The configuration and arrangement of reinforcing in the specimens are shown in Fig. 2. Four one-eighth scale core wall specimens were tested. Each specimen represented the core walls of the lower three stories of a high-rise building of approximately twenty five stories. The configuration and arrangement of longitudinal and transverse reinforcement of the four specimens were identical. The specimens had rectangular cross sections measuring  $90 \times 900$ mm, were 700mm in width and had a shear span ratio of 2.5. D10 and D6 deformation bars with a yield strength of 360.7MPa and 381.4MPa were used for longitudinal and transverse reinforcement respectively. High-strength bar U5.1 with a yield strength of 1314.6MPa was used for the confining bars. Specimen cover concrete was 5mm thick. The maximum aggregate size was 13mm and specified design concrete strength was 588MPa. The physical properties of the concrete and reinforcing are listed in Table 1.

The specimens were designed so that the shear strength would be larger than the flexural strength. Specimen 1 had no confining reinforcement. Specimen 2 was confined at the corner using closed reinforcement in contrast to Specimen 1. Specimens 3 and 4 were confined at the area near the corner using tie bars. Specimen 4 had twice the number of tie bars as Specimen 3. The confining bars were arranged up to a height corresponding to the second floor level (h:615mm).

### Test Procedures

The loading tests were conducted as shown in Fig. 3. In the lateral loading tests, the specimens were subject to forces by an actuator connected to the reaction wall. A constant axial loading force was applied by hydraulic jack over the specimen to represent the axial stress in the stage of coupling beam yielding at the center core. The axial stress was 60% of the concrete compressive cylinder strength at the positive loading for which the corner area is compressive, and 78.5kN at the negative loading respectively. The axial loads of Specimens 1, 2, 3 and 4 were 4825, 6610, 6512 and 6080kN respectively.

The loading was controlled by the horizontal drift angle at a height corresponding to the second floor level (h:615mm). The loading was cyclic lateral loading at  $R(\text{a drift angle}) = 1/1000(\text{rad.})$  (1cycle),  $2/1000$  (2 cycle),  $5/1000$ ,  $7.5/1000$ ,  $10/1000$ (1cycle respectively).

Table 1. Material Properties

Concrete				Steel				
Specimen	Compressive Strength $\sigma_c$ (MPa)	Young's Modulus* ( $\times 10^4$ MPa)	Split Strength (MPa)	Bar Size	Yield Strength (MPa)	Maximum Strength (MPa)	Young's Modulus ( $\times 10^5$ MPa)	Elongation (%)
NO. 1	52.6	2.97	3.74	D10	360.7	518.9	1.85	18.2
NO. 2	71.9	3.52	4.51	D6	381.4	524.9	1.90	20.9
NO. 3	70.9	3.40	4.82	U5.1	1314.6	1397.5	1.91	7.5
NO. 4	66.2	3.52	3.31					
comp. test	62.9	3.49	3.61					

\* Secant Modulus at one-third of  $\sigma_c$

Yield Strength of U5.1: 0.002 off set

Table 2. Test Results

Specimen	Flexural Cracking		Maximum Strength				Limit Drift Angle
	Load (kN)	Drift Angle ( $\times 1/1000$ rad.)	Exp. Load (kN)	Cal. Load (kN)	Eep/Cal	Drift Angle ( $\times 1/1000$ rad.)	( $\times 1/1000$ rad.)
NO. 1	62	0.5	464	362	1.28	4.4	4.6
NO. 2	73	0.4	377	440	0.86	3.1	3.1
NO. 3	53	0.4	489	436	1.12	4.4	6.0
NO. 4	56	0.3	557	417	1.34	7.8	9.6

Limit Drift Angle: Maximum drift angle which specimen keeps 80% of maximum strength

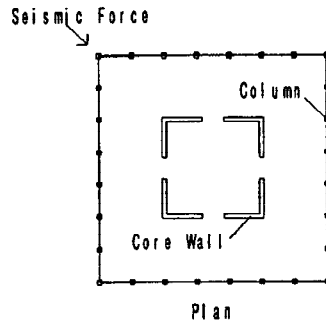


Fig. 1 Core Wall System High-rise Building

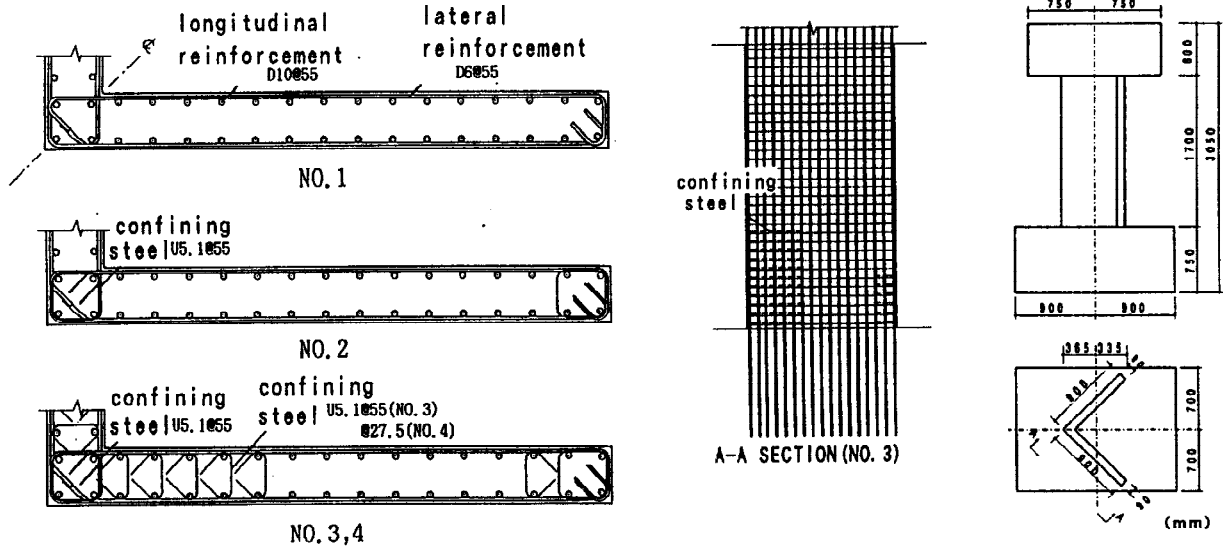


Fig. 2 Test Specimens

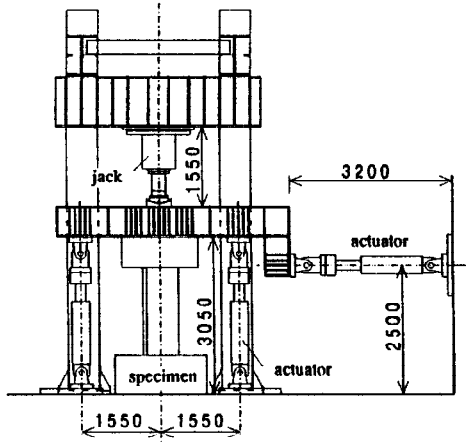


Fig. 3 Loading System

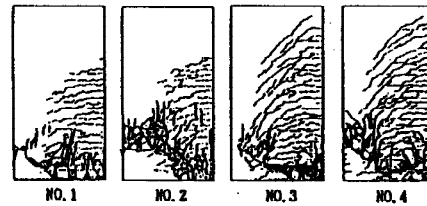


Fig. 4 Crack Patterns

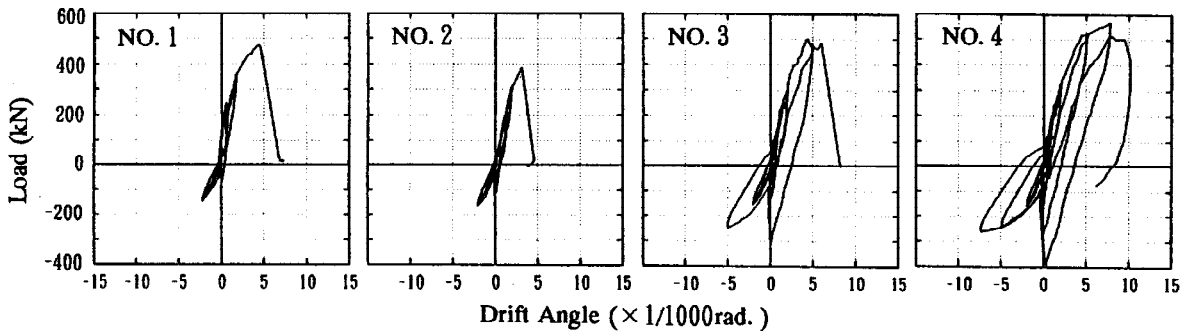


Fig. 5 Load-Drift Curve

## Test Results

**Fracture process** The test results are listed in Table 2. The crack patterns of specimens during the final stage are shown in Fig. 4. In Table 2, the flexural cracking loads and the maximum strengths represent values at negative loadings and positive loadings respectively. At the positive loadings of all specimens, the longitudinal reinforcement at the compressive end yielded at cycle  $R=1/1000$ , and the corner area appeared to crack vertically and crumbled a little by cycle  $R=2/1000$ . At the negative loadings, flexural cracks had occurred by  $R=1/1000$ . At the final stage, all specimens crumbled and the strength decreased at the positive loadings. As regards the maximum strength, except for specimen 2, the experimental results were larger than calculated by the equations previously mentioned (AIJ, 1990).

**Load deflection curves** Fig. 5 shows the load deflection curves. In the figure, the load deflection loops are discontinuous as the axial loads were changed at  $R=0$ . In the case of specimens with confining reinforcement, the limit drift angle of specimens 3 and 4 which were confined at the corner and the area near the corner, was larger than that of specimen 2. Specimen 2 was confined at the corner only. The limit drift angle of specimen 4 which has more confining reinforcement than specimen 3, was larger than that of specimen 3. These results show the effectiveness of concrete confinement. The drift angle of specimen 1 which has no confining reinforcement, was larger than that of specimen 2 which has confining reinforcement at the corner. The reasons for these results is discussed in another chapter.

**Strain distribution of confining reinforcement** Fig. 6 shows the confining reinforcement strain distribution at the bottom of specimens 3 and 4. Specimen 4 had twice the number of (half the vertical pitch of) tie bars at the area near the corner as Specimen 3. The strain was measured by strain gauges attached to both sides of the confining reinforcement at the neutral axis, and the values of strain were the average of both sides. In the figure, point A is a measuring point of closed reinforcement, and points B, C, D, E were

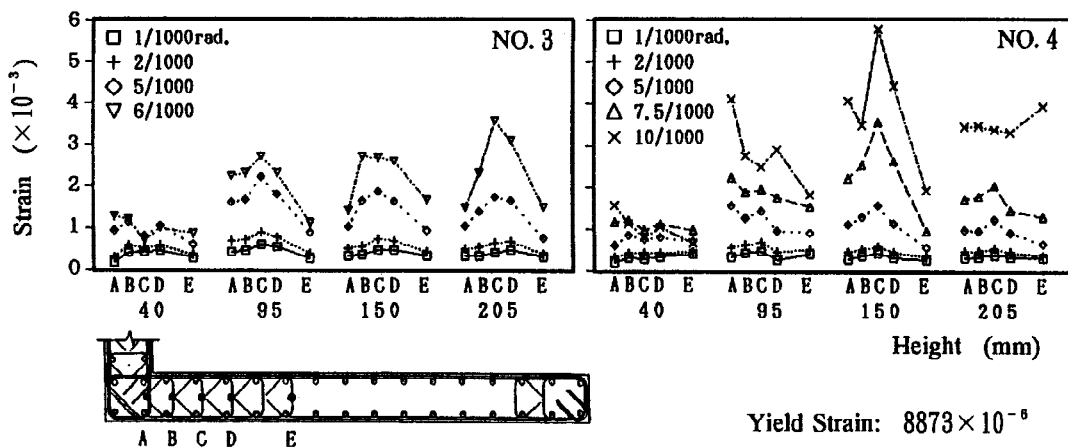


Fig. 6 Strain Distribution of reinforcement

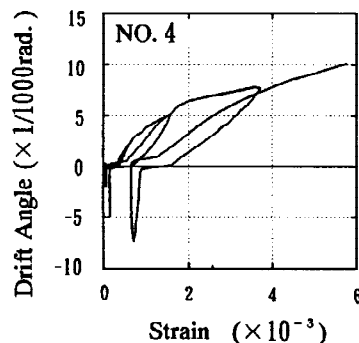


Fig. 7 Confining Reinforcement Strain versus Drift Angle

the measuring points of tie bars. The distribution was the longitudinal distribution in the cross section of the wall at heights of 40, 95, 150, 205mm, and at the peak of positive loading (the constant axial stress was 60% of the concrete compressive cylinder strength) of each drift angle.

Strain increased with increase in drift angle at all measuring points in both specimens 3 and 4. As all values of strain were lower than yield strain ( $8873 \times 10^{-6}$ ), an increase in confining reinforcement strain reflects an increase in confining stress. Therefore, it is believed that an increase in confining reinforcement strain indicates an increase of confinement effect by confining reinforcement with increase in drift angle, when the compressive stress of concrete near the measuring points increases. The strain of specimen 3 was larger than that of specimen 4 at each drift angle. This means that a confining force by the confining reinforcement of specimen 3 was larger than that of specimen 4. On the other hand, specimen 4 had twice the number of tie bars as Specimen 3. Therefore, it is believed that the confining force by the unit cross section area of specimen 4 was larger than that of specimen 3 and high confining force was the reason that the limit drift angle of specimen 4 ( $R=9.6/1000$ ) was larger than that of specimen 3 ( $R=6/1000$ ). The increase of confining reinforcing strain with increase of drift angle of specimens 3 and 4 was pronounced from  $R=5/1000$  to  $6/1000$ , and from  $R=7.5/1000$  to  $10/1000$  respectively, approximately the final stage of both specimens.

With regard to the effect of height from the base on strain distribution, the values at a height of 40mm ( $\approx 0.5t$ ,  $t$ : thickness of the wall, 90mm) were small compared with the values at other heights of both specimens 3 and 4. The reason for this result seems to be the effect of confining by the base. Before  $R=5/1000$ , the values at height of 95mm ( $\approx t$ ) were the largest, and the value decreased a little with increment of the height (150, 205mm) for both specimens 3 and 4. On the other hand, after  $R=5/1000$ , the values at a height of 150mm ( $\approx 1.5t$ ) were the largest. As for the strain distribution at each height, the values of point B and C were the largest and that at point E was the smallest. However, at a height of 95mm for specimen 4, the value of point A on closed reinforcement was largest after  $R=5/1000$ . Fig. 7 shows strain - drift angle relationship at point A which is located at a height of 150mm for specimen 4. In the figure, strain of confining reinforcing increased with the increment of the drift angle at the positive loading when the high axial load was applied.

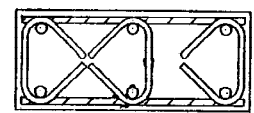
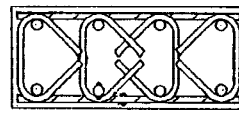
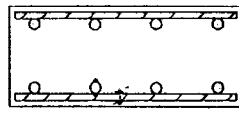
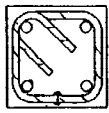
## COMPRESSION TESTS

### *Test Specimens*

Twenty nine specimens (see Fig. 8, Table 3) were tested. Nine square section specimens (C0~ C2) and twenty rectangular section specimens (W0~ W7) simulated the corner and the area near the corner of the core wall specimens respectively. Two or three specimens were made for the arrangement of reinforcing.

For example, specimens C11, C12, C13 were made as specimen C1. With regard to the square section specimens, specimen C1 simulated the corner of the core wall specimen 1, and normal strength bars with a yield strength of 381.4MPa were used for hoops. Specimen C simulated the corner of specimens 2, 3 and 4, and high strength bars with a yield strength of 1314.6MPa were arranged on the normal strength bars.

The parameter of the rectangular section specimens was the number of confining tie bars. With regard to specimens W1~ W5, the number of tie bars was varied by the vertical (compressive axial direction) pitch of tie bars. The specimen W1 simulated the area near the corner of core wall specimens 1 and 2, and the specimens W3 and W4 simulated that of specimens 3 and 4 respectively. Specimens W6 and W7 were the specimens whose horizontal pitch of tie bars varied from that of the specimens W1~ W5. The



Section 90mm × 90mm

C0: no Reinf.

C1: Transverse Reinf. @55  
(normal strength)

C2: Transverse Reinf. @55  
(normal strength)

Confining Reinf. @55  
(high strength)

Section 90mm × 210mm

W0: no Reinf.

W1: no Confining Reinf.

W2: Confining Reinf. @73

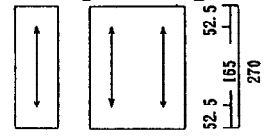
W3: Confining Reinf. @55

W4: Confining Reinf. @27.5

W5: Confining Reinf. @19

W6: Confining Reinf. @55

W7: Confining Reinf. @27.5



C0~C2 W0~W7  
Measuring System

Fig. 8 Test Specimens

Table 3. Test Specimens

Specimen	C01	C02	C03	C11	C12	C13	C21	C22	C23	W01	W02	W03	W11	W12	W13
Maximum Load (kN)	335	360	377	436	451	481	477	485	517	919	965	958	1088	1116	1108
Strain at Max. Load (%)	0.23	0.29	0.27	0.45	0.54	0.38	0.88	0.88	1.27	0.25	0.24	0.27	0.26	0.23	0.23

Specimen	W21	W22	W31	W32	W33	W41	W42	W43	W51	W52	W61	W62	W71	W72
Maximum Load (kN)	1170	1218	1255	1099	1218	1172	1137	1292	1250	1386	1059	1186	1134	1094
Strain at Max. Load (%)	0.24	0.26	0.40	0.28	0.35	0.44	0.43	0.50	0.72	0.56	0.29	0.30	0.38	0.34

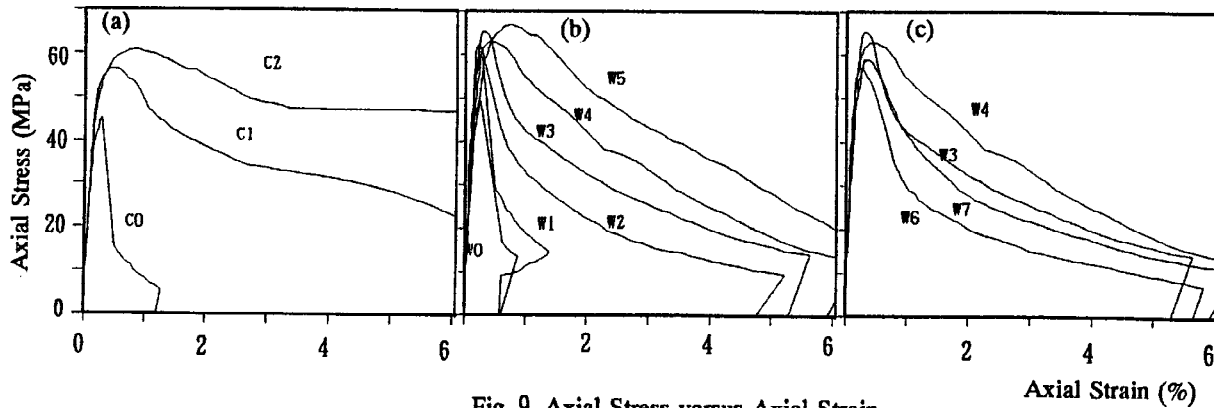


Fig. 9 Axial Stress versus Axial Strain

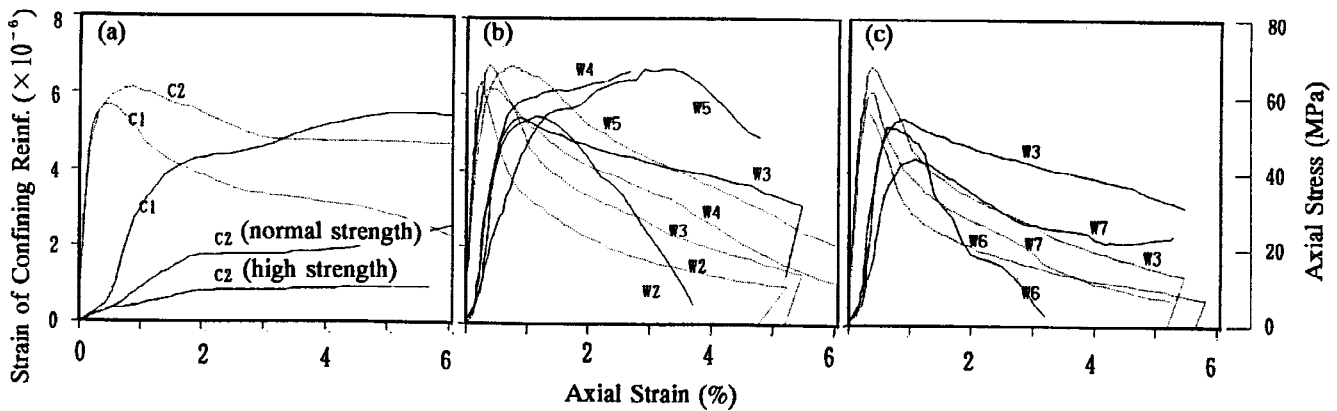


Fig. 10 Strain of Confining Reinforcement versus Axial Strain

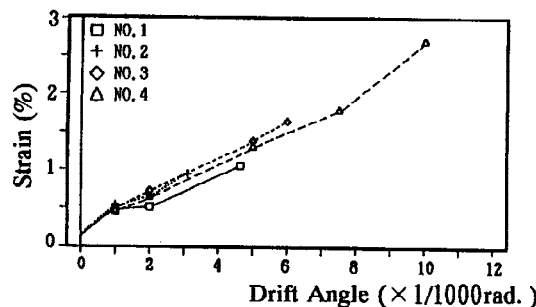


Fig. 11 Drift Angle versus Compressive Strain at Bottom of Core Wall

vertical pitch of tie bars of W6 and W3, W7 and W4 were identical. Specimens C0, W0 had no reinforcement. The specimens were made from the same materials as the specimens used in the core wall lateral loading tests.

### *Test Procedures*

Test specimens were subject to monotonic uni-axial compression. Axial strain was measured by transducer (see Fig. 8 for measuring length). Strain gauges were attached to confining reinforcement, transverse reinforcement and longitudinal reinforcement.

### *Test Results*

Fig. 9 shows the relationship between specimen axial compressive stress  $\sigma$  ( $=N/A$ , N:axial load, A:section area) and axial strain. In the figure, stress-strain curves show the results of specimens whose maximum stress was the second largest in the same reinforcement arrangement specimens. In Fig. 9(a), the maximum and post-failure stress of square section specimens with high strength closed reinforcement was much higher than the stress of specimens without such reinforcement. In Fig. 9(b), it is believed that the drop in stress after the maximum of rectangular section specimens with tie bars were smaller corresponding to increment of the number of tie bars. In Fig. 9(c), the maximum stress decreased and the drop in stress after the maximum increased with decrement of the number of tie bars by widening the horizontal pitch.

Fig. 10 shows the relationship between the strain of confining reinforcement and the axial strain of the specimens. Dashed lines in the figure show the relationship between the axial stress and the axial strain of identical specimens. In Fig. 10(a), the strain of the specimen C1, which had only the normal strength hoops, increased markedly with the starting of stress decrement. On the other hand, the strain increment of normal strength hoops for specimen C2, which also had high strength hoops, was not marked as that of specimen C1. In Fig. 10(b), the strain of the confining reinforcement was larger with decreasing of the stress loss after the maximum by the increment of the amount of confining reinforcement. As the values of strain were lower than yield strain ( $8873 \times 10^{-6}$ ), it is believed that confining reinforcement worked more effectively with increasing amounts. In Fig. 10(c), it is believed that the confinement effect for specimens W6, W7, whose horizontal pitch was wider, was lower than for other specimens.

## ANALYSIS TEST RESULTS

### *Confinement at the Corner of Core Wall Specimens*

During the lateral loading tests of core wall specimens, the limit drift angle of specimen 1 without confining reinforcement was  $R=3.1/1000$ , which was lower than that of specimen 2 ( $R=4.6/1000$ ) with confining reinforcement at the corner. On the other hand, in the compression tests using the square section specimens which simulated the corner of the core wall specimens, improvement of compressive ductility by the confining reinforcement was pronounced. Therefore, it is believed that the effect of axial load was larger than improvement of compressive ductility. Namely, as the ratio of axial stress to the concrete compressive cylinder strength was made constant during the lateral loading tests, specimen 1, for which concrete strength was lower than that of other specimens, was subject to the lowest axial load. It is believed that the low axial load was the reason for the higher deformation capacity of specimen 1 than specimen 2.

### *Confinement at the Area near the Corner of Core Wall Specimens*

In the core wall specimens with confining reinforcement, the limit drift angles of specimens 4, 3 and 2 were  $R=9.6/1000$ ,  $6.0/1000$  and  $3.1/1000$  respectively. On the other hand, in regard to the compressive ductility of compression tests, specimens which simulated the area near the corner of core wall specimens, the highest was specimen W4, followed by specimen W3, and the lowest was specimen W1. As the specimens W4, W3 and W1 corresponded to the core wall specimens 4, 3 and 2, it is believed that the concrete confinement of the area near the corner of the core wall was effective in improving the deformation capacity of the core wall and the effectiveness was the results of improvement of the compressive ductility of the confined area.

### *Core Wall Base Compressive Strain*

Fig. 11 shows the relationship between the drift angle and compressive strain at the bottom of the core wall specimens. The strain was measured with a transducer located 35mm inside the compressive edge of the specimen, and the measuring length was 105mm. Compressive strain increased in proportion to the drift angle, and the maximum compressive strain became larger as the limit drift angle of the specimen increased. As mentioned before, the compressive ductility increased as the corner or the area near the corner were confined. Therefore, it is believed that area which is more confined could resist the compressive stress until the higher level of compressive strain, and as a result, the limit drift angle of the core wall increased.

## CONCLUSIONS

Lateral loading tests of core walls using concrete of 60 MPa compressive strength were conducted with concrete confinement at the corner or the area near the corner as parameters. Compression tests with specimens which simulated the corner or the area near the corner of the core wall were also carried out. Major findings are as follows;

- (1)The concrete confinement by confining reinforcement at the area near the corner had a significant effect on improvement of the deformation capacity of the core wall.
- (2)From the results of the compression tests, it was found that the improvement of compressive ductility of the confined area improved the deformation capacity of the core wall.
- (3)The closed confining reinforcement of high strength was effective in improving the deformation capacity of the core wall.
- (4)The compressive strain at the extreme end of the bottom of the core wall was approximately proportional to the drift angle, and the maximum strain increased with the increment of the limit drift angle.

## REFERENCES

Architectural Institute of Japan (1990). *Ultimate strength and deformation capacity of buildings in seismic design (in Japanese)*, 396-397, Japan.